

---

# 4

## Chapter

### Manufacturing and assembly

*Manufacturing and assembly are intricate to the mechanical design of an induction machine (IM) rotor and were considered throughout the entire design process. Chapter 4 includes a detail description on the processes followed to produce the intricate IM rotor section. In the chapter it will become apparent how the manufacturing and assembly of each component influences the entire design. Both a failed and successful manufacturing and assembly attempt are described.*

#### **4.1 Methodology behind designing for manufacture and assembly**

As mentioned throughout the dissertation, design for manufacture and assembly (DFMA) is critical in order to design something that can be manufactured and assembled. Due to the intricate nature of a laminated-caged IM rotor, the assembly becomes even more critical. In some cases the design had to be revised in order to enable the rotor to be manufactured and assembled.

The following sections will discuss the process in detail, however, the basic idea is to laser cut the lamination discs and clamp the stack using the spacers at each end. The clamped stack's ID and conductive bar slots are then machined to size. Followed by the assembly of the end rings and conductive bars into the lamination stack, after which the magnetic core is assembled onto the shaft. Finally the OD of the rotor is machined to size and the rotor is balanced. However simple this might sound, it was not the case and more than one component had to be remanufactured.

#### **4.2 Rotor manufacturing and assembly, first iteration**

During the discussion of the manufacturing and assembly procedure the manufacturing of the individual components are described followed by the description of the assembly. The mistakes made are illustrated and the lessons learnt are discussed.

##### **4.2.1 Manufacturing lamination discs**

The lamination material is in the form of a 0.35 mm sheet and depending on the quantity required, the lamination discs can either be laser cut or punched. Punching requires expensive tooling and therefore is only viable, when large quantities are required. The punched laminations also tend to have "burs" at the

sheared edges and might require additional rolling. Similar to sheet plate rolling, the process will ensure the lamination discs are the correct thickness.

For this particular design, mainly due to the quantity required and capability of the local supplier, the lamination discs are laser cut. However, the laser cut process cannot provide the required dimensional tolerance and is only capable of  $\pm 200 \mu\text{m}$ , nor can the process produce the required surface finish. Therefore, both the ID and bar slots are cut smaller than the final required dimensions and the OD is cut larger. This is to allow for accurate secondary machining, to the required dimension within the allowable dimensional tolerance.

Due to the axial length of the lamination stack and clamping spacers (158 mm), it was not advisable to attempt to accurately machine the twenty four, 10.1 mm bar slots, as one assembly. Not wanting to divide the stack into smaller stacks, the conductive bar slots are laser cut undersize to a diameter of 9 mm. This is done to allow the secondary machining of the entire stack, to be done at once. The idea is that the pre-cut slots will guide the drill and the slots will basically be reamed to size.

The reason the bar slot has to undergo secondary machining is not necessarily due to the required dimensional tolerance, but rather to obtain the required surface finish and correct slot position. Due to the fact that the maximum stress occurs at the root and tip of the bar slot, no stress concentrations due to surface finish are allowed at these positions. The position of the bar slots is also critical to allow for assembly of the conductive bars into the lamination stack. The laser cut disc is illustrated in Figure 4-1 with the detail drawing shown in Appendix B.

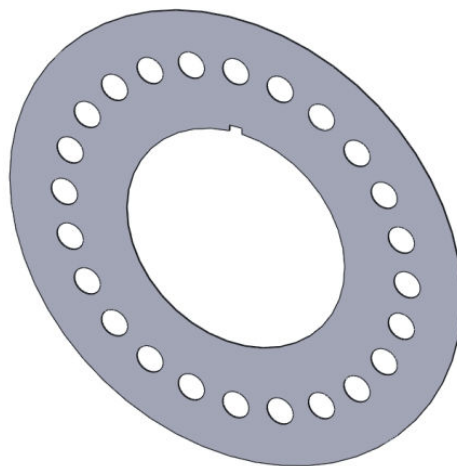


**Figure 4-1: Illustration of the laser cut laminations**

Figure 4-1 illustrates a lamination disc with the twenty four bar slots and shows the keyway on the ID, which is used to align the bar slots. However, due to the inaccuracy of the position and size of the keyway the bar slot alignment will not be adequate, therefore relying on the secondary machining process for the final bar slot positions.

The lamination stack requires an axial length of 150 mm, with a lamination disc of thickness 0.35 mm, it is calculated that at least 429 discs are required. Due to the complex geometry of a disc and the large amount required, the manufacturing became more expensive than the material itself.

#### 4.2.2 Manufacturing the spacer (clamping plates)

In order to machine the laminations, to the correct size it is stacked and clamped, the clamping is required to be ridged in order to achieve the required manufacturing tolerances. The clamping can be done in many ways, however, it was decided to use plates and threaded rods, which is discussed later. Except for the clamping function, the spacer also relieves the shear stress in the conductive bars as discussed throughout the literature and design chapter. Therefore the bar slots are required to be machined over-sized to a diameter of 11 mm. This is done to allow the bars to bend and enable secondary machining of the lamination stack's bar slots.

Due to the clamping function, the spacers cannot be removed in order to machine its ID separately. Consequently, the IDs of both the lamination stack and spacers are machined as one component, resulting in them having the same dimension. As discussed in section 3.7.4, this influences the material selection and a material with the same or greater modulus of elasticity  $E$ , is required to enable the use of the same amount of interference. After the machining of the clamped lamination stack's ID two extractable dowel pin holes are inserted at each side of the stack, to enable accurate end ring alignment, however, it is described in detail in section 4.2.6. The machined spacer is illustrated in Figure 4-2, with twenty four bar slots, eight M8 clamping-bolt-holes and the alignment keyway at the ID. The detail drawing is included in Appendix B.

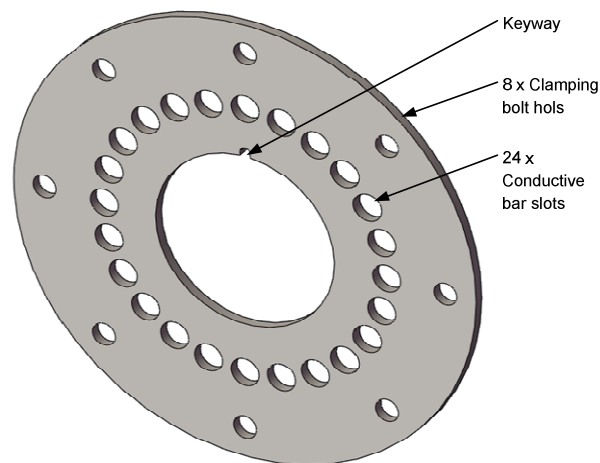


Figure 4-2: Illustration of the spacer (clamping plate)

#### 4.2.3 Manufacturing of the end ring

In some IM rotor section designs, the end rings and conductive bars are used to clamp the lamination stack, during the machining of the ID. Therefore, the end rings would have the same ID as the lamination stack. This presents a problem due to the fact that the aluminium end rings require an interference of

more than double that of the lamination stack. Consequently, the end rings are machined separately and assembled to the stack afterwards.

The end ring as illustrated in Figure 4-3 is machined with an oversized OD to accommodate two slotted dowel holes. The extractable dowels are used to ensure the bar slots of the lamination stack and end rings align, the extractable dowels are also used to ensure the ID's of the lamination stack and end rings are concentric. Consequently the position and size of the dowel slot is critical in order to achieve acceptable alignment. Extractable dowel pins are used to enable the extraction of the dowels before the OD is machined. The reason the dowel holes are slotted is due to the required temperature differential of the entire IM rotor section, during the assembly onto the shaft. The dowel holes are slotted 150  $\mu\text{m}$  radially to accommodate the relative radial expansion between the end rings and lamination stack. The radial clearance is taken up due to the relative radial growth and at the maximum temperature the dowel pin has no play and the end ring and lamination stack's ID is concentric. More detail on this is presented in section 4.3.5 and the detail drawings included in Appendix B, illustrates the slotted dowel hole in more detail.

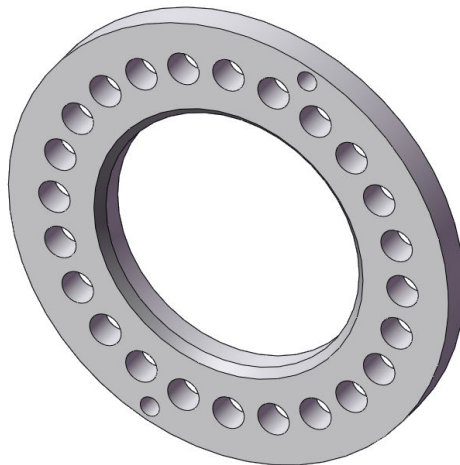


**Figure 4-3; Illustration of oversized end ring with dowel slots**

#### **4.2.4 Manufacturing of the conductive bars**

The conductive bars are manufactured to their final dimension and do not require any secondary machining process. From Figure 4-4 it is apparent that the entire bar is not the same diameter, this is done to minimize the manufacturing cost. Because only the two end sections of the bar requires a tight dimensional tolerance, due to the end ring/bar interface. The two end sections are also not machined to the same size. The normal parallel interference fit side is machined to a diameter of 10.02 mm and the 3 mm dowel insert side has a diameter of 9.99 mm. More detail can be seen from the detail drawings included in Appendix B.

Figure 4-4 also illustrates the 2.9 mm dowel hole required for the 3 mm dowel pin. The hole is drilled and then reamed to size with a precision grinded reamer. The effect of the large interference at the bar/dowel interface is described in the detail design section 3.7.5. The description also present practical

measured results, to ensure the bar will not fail during operation and to ensure a low electrical contact resistance is achieved.

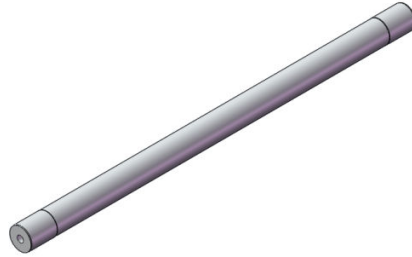


**Figure 4-4: Illustration of the conductive bar with a dowel hole**

#### **4.2.5 Manufacturing of the stacking mandrel with a keyway**

As mentioned throughout the assembly procedure, the individual lamination discs will have to be stacked and undergo secondary machining. The decision was made to assemble the entire 150 mm lamination stack and machine it as one component. For this, a stacking mandrel is required to ensure the lamination discs are aligned concentrically and the addition of the key, will ensure the bar slots are aligned. The shoulder included onto the mandrel will ensure the lamination stack is perpendicular to the mandrel surface. After satisfactory alignment of the individual lamination discs and clamping spacers, the mandrel is used to hold and set up the assembly for the secondary manufacturing processes.

However, due to a difference in the lamination disc's ID of about 400  $\mu\text{m}$ , due to dimensional tolerance, the mandrel has to be machined to accommodate all disc sizes. Consequently, a loose sliding fit is found in most instances and therefore resulted in some misalignment of both the IDs and bar slots. Figure 4-5 illustrates the mandrel with the keyway and the detail drawing is included in Appendix B.

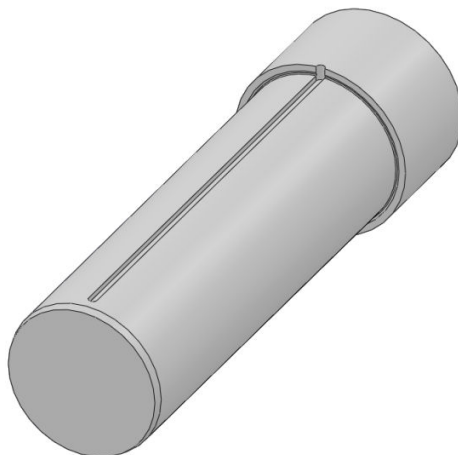


**Figure 4-5: Lamination stacking mandrel with keyway**

#### 4.2.6 Assembly of lamination stack

The individual lamination discs are stacked onto the mandrel with the key ensuring angular alignment. One spacer is assembled on each side of the lamination stack and the M8 bolts are used to axially clamp the stack as illustrated in Figure 4-6. After measuring and ensuring the axial dimension of the assembly is correct, the assembly is ready for its secondary machining process. The mandrel is used to clamp and set up the assembly for machining where the extractable dowel holes are inserted and the bar slots machined to size.

The 9 mm diameter lamination bar slots are required to be machined to 10.1 mm and this process was attempted on a computer-numerical control (CNC) milling machine. The first step was to setup the assembly to ensure the secondary machining could be done from the correct reference. After the setup of the assembly, the bar slots were drilled to 9.8 mm and reamed to the final diameter of 10.1 mm.

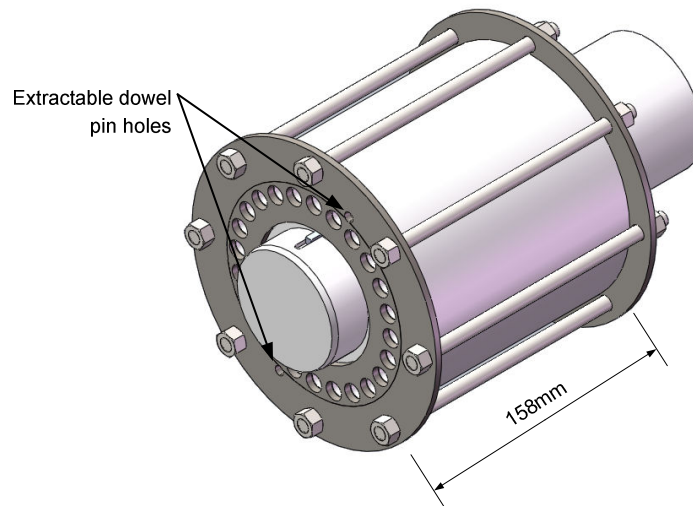


**Figure 4-6: An illustration of stacking the mandrel and clamping the lamination stack**

After final reaming of the bar slot a visual inspection revealed that the secondary machining process was unsuccessful. The bar slots were no longer round and their position, relative to each other and the ID of the stack was altered significantly. The inspection also showed that the surface finish was jagged and it indicated that the machining process only removed material on some parts of the slot. The problem seemed to worsen as the depth of the slot increased. The slot geometry and position deteriorated to such an extent, that the decision was made to scrap the lamination stack. The assembly process was halted and had to be revised before the new lamination discs could be ordered.

#### 4.2.7 Lessons learnt

After consulting with several advanced machining facilities the conclusion was made that the assumption that the laser cut slots would guide the drill and reamer was grossly wrong. The low stiffness of the long drill and reamer ( $\pm 200$  mm) was thought to be an advantage, in the sense that it would follow the laser cut slots. However, this was not the case and together with the misalignment between

the tool and slots, the position and geometry of the slots were altered. Both the drill and reamer drifted due to the low stiffness and the long axial stack length.

However, the process might have been more successful if a loose head tool holder was used to hold the tool. This would have allowed the drill to follow the laser cut slots more accurately. The setup of the assembly in the CNC milling machine would also have been less critical and the misalignment would have been reduced.

The indication from the manufacturing specialists was that the axial length of the stack was too long and it would have to be sub-divided into smaller stacks. The main reason would be to use a standard length tungsten carbide cutting tool to ensure accurate size and positioning of the slots. The lamination disc therefore requires no pre-cut bar slots or clamping holes. Reducing the laser cut process cost considerably due to the reduction in detail.

### 4.3 Rotor manufacturing and assembly revised iteration

Using the lessons learnt from the first manufacturing and assembly process, a new revised process is formulated in conjunction with some manufacturing specialists. The main problem is ensuring the bar slot's geometry and relative positioning is correct. With only a new lamination stack required, the spacers, end rings and conductive bars will be reused.

The revised process entails using five smaller lamination stacks of 30 mm each, clamped with 10 mm end plates and machining the bar slots and IDs to their final dimensions. The individual stacks, spacers, conductive bars and end rings can then be assembled. The process is explained in detail throughout this section.

#### 4.3.1 Laser cut laminations

The fact that the new lamination discs have no bar slots, clamp holes or a keyway, reduces the price of the manufacturing considerably. Figure 4-7 illustrates the solid ring as used to stack in smaller 30 mm stacks.

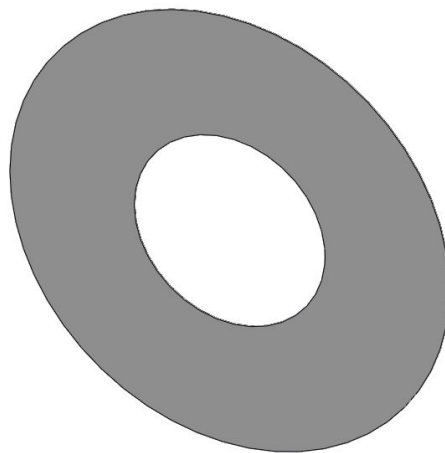


Figure 4-7: Illustration of solid lamination disc

The lamination ring is laser cut with an ID of 70 mm and the OD of 175 mm. This is to allow for secondary machining, as with the first iteration. However, the outer diameter of the lamination disc is increased, in order to improve the clamping of the small stacks as well as the complete 158 mm lamination stack. From Figure 4-6 it can be seen that the clamping on the OD of the assembly would have been difficult and it would have influenced the manufacturing dimensional tolerances obtained.

#### 4.3.2 Manufacturing of the five lamination stacks

Five 30 mm lamination stacks are made up with a 10 mm end plate on each side. The stacks are held in position and the eight M8 clamping bolt holes are drilled and the stacks are clamped using the M8 bolts. The ODs of the stacks are cut on a lathe so the surface can be used as a reference for the machining of the stack's ID. With the OD as the reference surface the ID is machined on a lathe and precision grinded in a temperature controlled room. The stacks are then individually set up in a CNC milling machine, where the ID is used as reference to precisely position the bar slots, dowel holes and alignment hole as illustrated in Figure 4-8.

The extractable dowels would have the same function as discussed earlier, which is to align and hold the end rings in position. The addition of the alignment hole is to ensure accurate bar slot alignment between the individual lamination stacks. This will be done using an alignment rod, precisely machined to have a tight sliding fit.

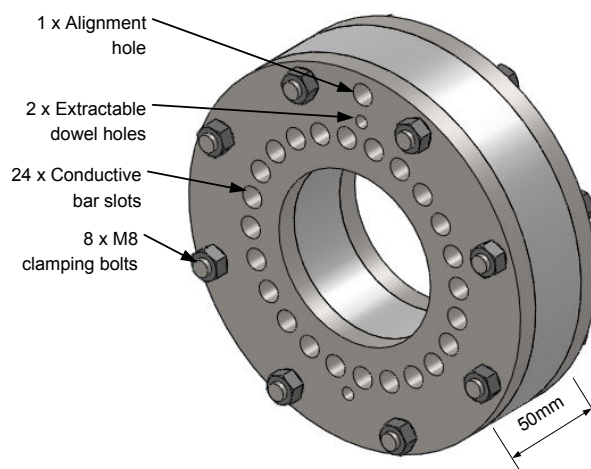


Figure 4-8: Illustration of 30 mm lamination stack after machining

#### 4.3.3 Assembling the smaller lamination stacks onto a mandrel

The biggest drive behind the decision to machine the entire 150 mm lamination stack as one assembly is to ensure the precise alignment of the ID and bar slots of each lamination disc. Consequently, after dividing the stack into five smaller stacks, the biggest challenge is to ensure the precise alignment of both the ID and bar slots of each lamination disc.

To ensure the alignment is good enough, a mandrel is required with a precision sliding fit for the lamination stacks. The mandrel is similar to the previous mandrel as illustrated in Figure 4-5 apart from the diameter and without a keyway. With the individual lamination stacks completed, epoxy is used to glue the laminations together and hold everything in place. The glue is applied to the side of the lamination stacks and after an adequate amount of time the end plates are removed. Great care is taken to ensure the lamination discs do not move as the stack is assembled onto a chilled mandrel. The mandrel is chilled to ensure the stacks are easily assembled without allowing a large clearance that could influence the alignment.

After all five stacks are assembled onto the mandrel, the alignment rod is inserted into the alignment hole. The spacers and eight M8 rods as illustrated in Figure 4-9, are used to clamp the 150 mm stack in order to remove the mandrel. However, as the mandrel was pressed out the bottom spacer got stuck and was deformed, so much so that the component had to be scrapped. The mandrel is shown in Figure 4-10 and illustrates the material that was removed due to the spacer.

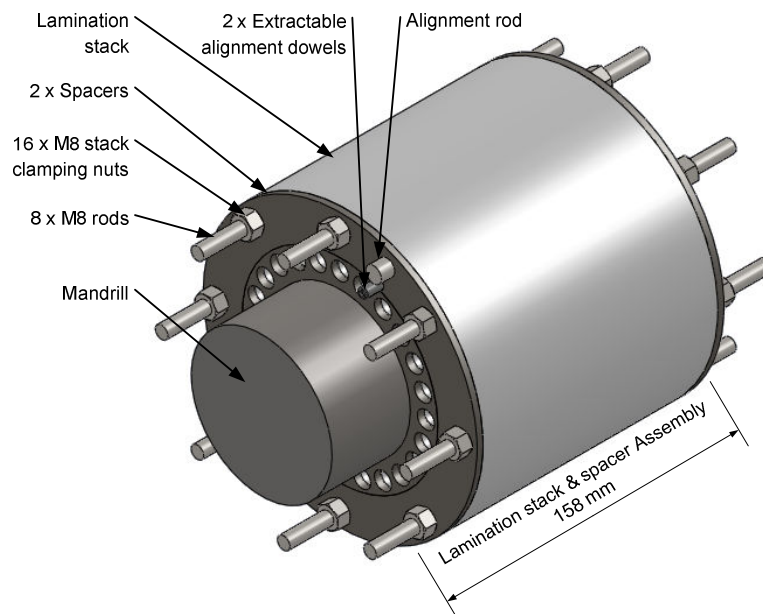


**Figure 4-9: Illustration of the assembled and clamped second lamination stack**



**Figure 4-10: Illustration of the jagged mandrel surface due to the bottom spacer removing material**

Consequently a new spacer had to be manufactured and the final ID of the new spacer was not exactly the same as the scraped spacer due to dimensional tolerances. The lamination stack was glued on the outer surface and the new spacer was assembled without any relative movement between the other components in the assembly. The extractable dowel pins enabled the precise alignment of the new spacers ID and slots relative to the lamination stack. The difference in interference between the two spacers is illustrated by the calculated contact pressure as shown in Table 5-2.

#### 4.3.4 Squirrel cage assembly

With the complete 150 mm lamination stack assembled and clamped using the spacers and M8 rods, the squirrel cage is assembled. First the one end ring is put in position using two extractable dowels and a clamping ring is employed to clamp the end ring axially as indicated in Figure 4-11. After securing the one end ring, the conductive bars are individually cooled in liquid nitrogen and shrink fitted into the end ring. After all twenty four conductive bars were shrink fitted, the second end ring is slid into position. The reason the second end ring cannot be shrink fitted, is because of the small diameter of the bar and large interference at the bar/end ring interface.

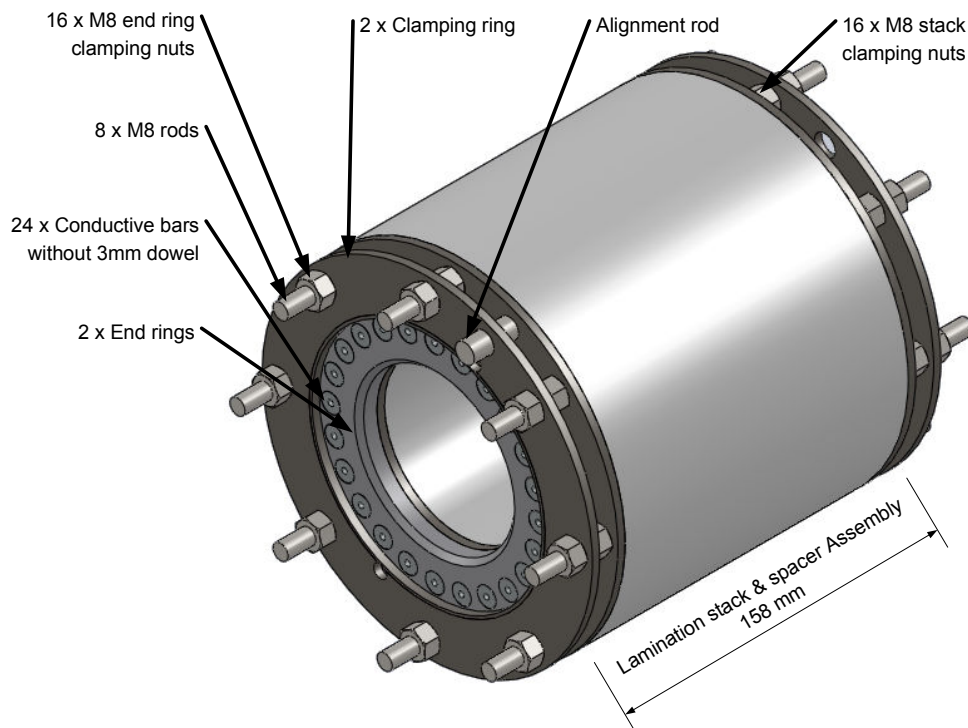


Figure 4-11: Illustration of clamped IM rotor section

In order to explain this consider (4.1), where the relative change in diameter  $\Delta d$  can be calculated, when the material's thermal expansion coefficient  $\alpha$ , change in temperature  $\Delta T$  and original diameter  $d$  is known [42]. From this it can be seen that in order to overcome the  $15\mu\text{m}$  radial interference at the bar/end ring interface the end ring's temperature increase is calculated to be  $\Delta T = 130\text{ }^\circ\text{C}$ . However, the pitch circle diameter (PCD) of the bar slots will increase from 110.0mm to about 110.33mm.

Consequently resulting in misalignment between the bar slots and conductive bars, that will make, assembling the end ring impossible. Furthermore, the temperature difference of  $\Delta T = 130\text{ }^{\circ}\text{C}$  is not adequate and is more likely to be in the region of  $\Delta T = 200\text{ }^{\circ}\text{C}$ , in order to freely assembly the bar into the end ring.

$$\Delta d = \alpha \Delta T d \quad (4.1)$$

Furthermore, the reason both end rings aren't shrink fitted is not only due to the slot and bar misalignment problem. It is also due to the process followed in order to assemble the complete IM rotor section onto the shaft, which is discussed in detail in section 4.3.5.

Press fitting the end ring/bar connection is also not an option, due to the risk of the removal of material. This will in effect reduce the amount of interference, therefore, increasing the contact resistance and reduce the machine's efficiency.

Consequently, as mentioned throughout the detail mechanical design the one end ring's interference fit at the end ring/bar interface is only done after the entire assembly is assembled onto the shaft. This is done by forcing the 3mm dowel into the 2.9mm hole in the conductive bar and is discussed in more detail during section 4.3.6.

#### 4.3.5 Shrink fitting the IM rotor section

The complete rotor section assembly as shown in Figure 4-11 is assembled onto the shaft. During the shrink fit process the interference must be overcome and this can be done by either cooling the inner component or heating the outer component. Due to the complexity of the IM rotor section the best method of assembly is probably by cooling the shaft and heating-up the rotor section to about its operating temperature. However, there are many factors to be considered and this shrink fit is quite a unique problem.

Firstly, the clearance required at the interface to freely assemble a component is critical. The amount of clearance is very much dependent on the size, geometry, and surface area of the component to be shrink fitted. A small component with a relatively large surface area would tend to return to the ambient temperature much quicker than for instance a large component with a relatively small surface area. The result is the percentage clearance required, relative to its size, would be more for the small component compared to that of the large component. Consequently calculating the amount of clearance required for a shrink fit is not a trivial exercise. In fact the entire shrink fit process is nerve-racking especially if the temperature differential is limited by external factors and the components are relatively big and heavy, making it difficult to manoeuvre.

From experience, at least a  $100\text{ }\mu\text{m}$  radial clearance is required at the time the components are removed from the heat/cooling source. Furthermore, the heat/cooling source is required to be next to the assembly point, to ensure minimum loss in dimensional clearance.

The first method of shrink fitting investigated is; cooling the shaft considerably and only increasing the IM rotor section's temperature to its operating temperature. This way no special modifications or extra

calculations are required to ensure the IM rotor section is not over-stressed during the assembly process. With the laminations having the minimum thermal expansion coefficient ( $\alpha$ ) of  $12 \cdot 10^{-6}/^{\circ}\text{C}$  and the maximum limiting temperature differential is  $60 \text{ }^{\circ}\text{C}$ . It is calculated that the IM rotor section's minimum radial expansion is  $30 \text{ }\mu\text{m}$ . Therefore the shaft should be cooled enough to make up the remaining  $105 \text{ }\mu\text{m}$ <sup>12</sup> required.

The calculations indicate that the shaft should be cooled to about  $-200 \text{ }^{\circ}\text{C}$ , using Liquid Nitrogen. However, the dramatic cooling might quench the shaft material and could transform any retained austenite to martensite. Apart from the risk of the material being hard and brittle, there is also the risk of a change in volume due to the difference in densities between austenite and martensite structures. Manufacturing Engineering and Technology [13] states; a change in volume of up to 4% can be obtained due to the change in structure. A change in volume will alter the amount of interference, which will be unacceptable. Although the chances of having retained austenite is reduced by properly heat treated material, due to the high speed application quenching was too great a risk.

The second shrink fit assembly procedure investigated, is based on heating the IM rotor section to its maximum allowable temperature and slightly cooling the shaft. However, due to the large difference in thermal expansion coefficients of the materials in the assembly. A detailed stress analysis is required to investigate the maximum allowable temperature differential of the IM rotor section.

The facilities used for the shrink fit has a  $-60 \text{ }^{\circ}\text{C}$  fridge where the shaft is cooled, resulting in a radial shrinkage of about  $38 \text{ }\mu\text{m}$ . Consequently the IM rotor section is required to be heated-up to  $250 \text{ }^{\circ}\text{C}$  to obtain a required radial clearance of  $100 \text{ }\mu\text{m}$ .

Due to the difference in the bar's and lamination stack's thermal expansion coefficients, the large increase in temperature causes some material stress effects. In order to illustrate the significance of the rise in temperature; assume both ends of the bars are fixed to the end rings, allowing no relative movement between the bars and end rings.

From this scenario, the axial force  $F_T$  applied by the bar, due to the increase in temperature can be calculated using (4.2). The following parameters are required; the material's thermal expansion coefficient  $\alpha$ , modulus of elasticity  $E$ , change in temperature  $\Delta T$  and the cross-sectional area  $A$  [42].

$$F_T = \alpha \Delta T A E \quad (4.2)$$

From (4.2) the axial force is calculated to be  $F_T = 14542 \text{ N}$ . Using twenty four bars the total axial force is  $349 \text{ kN}$ , which is a significant force. Assuming the axial clamping have to support this type of load to ensure the correct axial length of the IM rotor section, the clamping components will have to be very strong. Take for instance the current eight M8 bolts used. The maximum stress would be  $1219 \text{ MPa}$ , therefore, resulting in a change in the axial length of the IM rotor section. Furthermore the clamping-rings, holding the end rings axially in position will most probably deform first and would have to be reinforced dramatically.

<sup>12</sup> Radial clearance required  $100 \text{ }\mu\text{m}$  plus lamination radial interference to overcome  $35 \text{ }\mu\text{m}$ , minus IM rotor section radial expansion of  $30 \text{ }\mu\text{m}$  equals  $105 \text{ }\mu\text{m}$  shaft shrinkage required.

However, the bars are not axially constrained at both ends. Due to the 3 mm dowel used to bring about the interference at the one end ring, being inserted only after the shrink fit of the IM rotor section is completed. The fact that the bars are free to expand axially, nullifies the stress due to an increase in temperature. Although the axial expansion is shown to have no effect a detailed FEM analysis is required to establish the total stress implications due to the temperature differential.

Figure 4-12 illustrates the Von Mises stress equivalent for the rotor section due to the temperature increase. In the simulation model, the lamination stack's axial length is reduced to 10 mm. This is done to reduce the number of mesh elements, to ensure a fine enough mesh can be used at the critical locations. The assumption will not influence the maximum stress calculated, because the conductive bars are free at one end as discussed in detail in the previous paragraph. Also the fact that the laminations, spacers and clamping rods have the same thermal expansion coefficients will result in no relative axial or radial growth between these components.

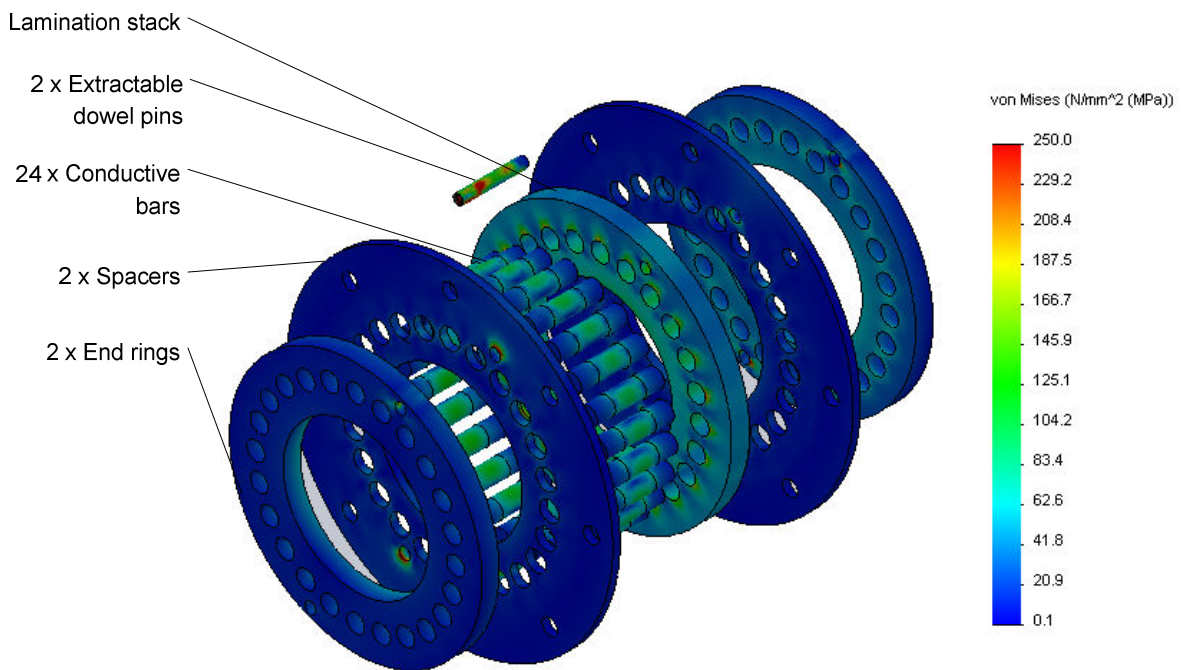


**Figure 4-12: IM rotor section stress due to heating up to 250 °C**

The critical locations are the extractable dowel pins and their interfaces, due to the relative radial growth between the end rings and the rest of the assembly. To compensate for this, the end ring's dowel holes are slotted radially, as discussed in 4.2.3.

The simulation results show a maximum stress of 250 MPa on the extractable dowel pins and their interface, however, the maximum stress is less than half the yield strength of the material. Therefore it is believed the IM rotor section can safely be heated-up to 250 °C, without yielding one of the component's materials. The addition of the slotted extractable dowel holes and the one free bar end ensures the IM rotor section is not over-stressed during the rise in temperature.

Figure 4-13 illustrates the shaft/IM rotor section assembly after the shrink fit was completed. The white top part of the shaft is ice that formed due to the cooling. The black on the outside of the IM rotor section is the adhesive used to glue the individual stacks.



Figure 4-13: Picture of the assembled IM rotor section onto the shaft

#### 4.3.6 Insert dowels into rod ends

After the assembly of the IM rotor section onto the, shaft the last things to do before machining the OD, was to create the interference fit at the end ring/conductive bar interface. This was done using a G-clamp and forcing each 3 mm dowel pin into the 2.9 mm hole in the bar, as illustrated in Figure 4-14 and Figure 4-15. The extractable dowel pins were also removed, so it does not interfere with the OD machining process.

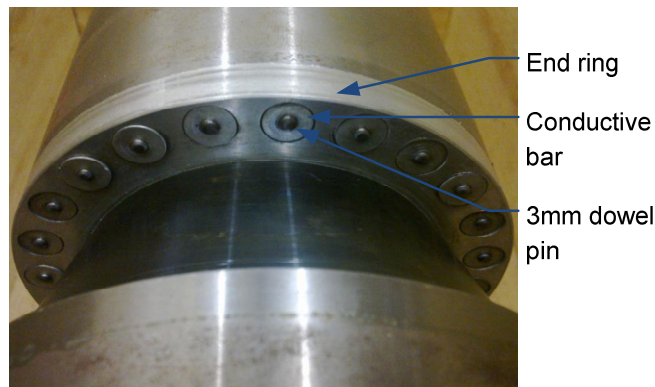


Figure 4-14: Inserting the 3mm dowel pins into the bars

The axial force  $F_a$ , required to force the dowel pin into the undersized hole, can be calculated using (4.3) [51]. The force is dependent on the interface diameter  $d_c$ , axial length  $l$  of the interface contact area, the contact pressure  $p_c$  at the interface and friction coefficient  $\mu$ . The friction coefficient has a significant

influence on the force and Machine Design Databook gives the value between 0.085 to 0.125 for lubricated surfaces and 0.05 for special lubricants [51].

$$F_a = \pi d_c l \mu p_c \quad (4.3)$$



**Figure 4-15: Illustration of the inserted 3mm dowel pins**

Using the nonlinear FEM calculated contact pressure at the 3 mm dowel pin/conductive bar interface and a friction coefficient of 0.125, the maximum axial force required is calculated as  $F_o = 1178$  N. The maximum stress on the conductive bar due to the axial force is calculated to be 15 MPa, which is extremely low. Due to the relatively small axial force buckling of the bar will not be a problem. Furthermore, the conductive bar will physically not be able to buckle under an axial load due to the lamination's-bar-slot, restricting the radial deflection.

#### 4.3.7 Machine final OD of entire rotor

The insertion of the 3 mm dowel pins concludes the IM rotor section assembly and the AMBs, inductive sensors and backup bearing spacer and sleeve could be shrink fitted onto the shaft. These shrink fits are relatively simple compared to the IM rotor section and no special stress calculations were required to establish the maximum allowable temperature differentials. The shaft with the assembled IM rotor section was kept at room temperature while the components to be shrink fitted were heated to the required temperature and the shrink fits were completed.

After all the components were shrink fitted to the shaft the IM rotor was ready for final machining. The rotor's OD was machined on a lathe and surface grinded to the required dimension. The grinding process is selected to minimise smearing of the lamination material as it influences the electromagnetic design negatively. After final machining the rotor is balanced and the end product is shown in Figure 4-16.

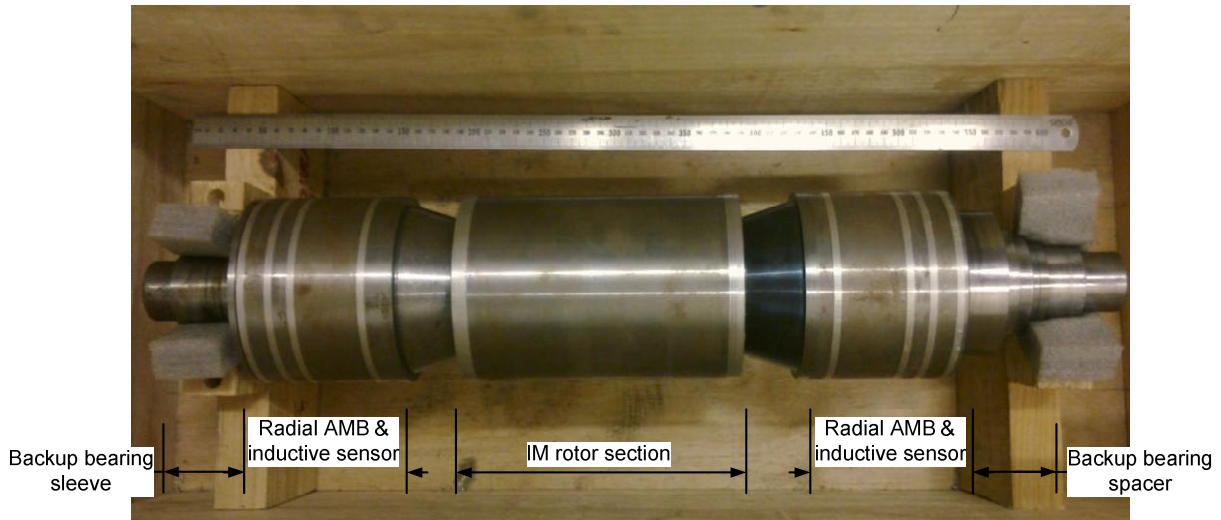


Figure 4-16: Illustration of the completed IM rotor

#### 4.4 Conclusion of assembly and manufacturing

Due to the inaccuracy of the laser-cutting ( $\pm 200 \mu\text{m}$ ) and the rough surface finish, the lamination discs required secondary machining. The discs could also not be machined to the required dimensional tolerance individually, therefore, the discs were stacked and clamped to be machined as one component. The first manufacturing and assembly iteration showed that the entire 150 mm stack could not be machined successfully as one component. This process also showed that the pre-laser cut slots were not a good idea. Apart from a huge increase in cost, the secondary drilling process could not be done successfully.

The revised manufacturing and assembly process, showed that five smaller lamination stacks can successfully be machined and assembled. This is done using a precision grinded stacking mandrel and alignment rod, to ensure ID concentricity and precise alignment of the bar slots. The lamination stack is then clamped using the spacers and threaded rods. The mandrel should be made of a material with a thermal expansion coefficient, greater than that of the lamination material, for instance AISI 304. This will ensure the mandrel can be extracted safely when the assembly is cooled and the mandrel shrinks, relative to the lamination stack.

Due to the difference in ID between the lamination stack and end rings, extractable dowel pins are employed to align the end rings. However, due to the required rise in temperature the dowel holes in the end rings are slotted. This allows the end ring to expand radially, without causing additional stresses due to the relative radial growth. The end ring is then clamped axially using a clamp ring to ensure there is no relative axial movement.

After the one end ring is in position, the conductive bars are shrink fitted and the remaining end ring is slid into position. Due to the slotted dowel holes in the end rings and the fact that the bar is free to expand axially, the IM rotor section can be heated in order to shrink fit the assembly.

A detailed stress analysis of the heated assembly was done to ensure none of the components are yielded during the temperature rise. After ensuring the temperature differential will not over stress the rotor section the IM rotor section was successfully shrink fitted onto the shaft. The 3 mm dowels were forced into position, the extractable dowels were removed and the rotor's OD was machined to its final dimension.

After the completion of the IM rotor the rotor was inspected and the entire IM could be assembled. The inspection process and findings are presented in the following chapter.

